Chapter 2. Artificial Atoms

Academic and Research Staff

Professor Marc A. Kastner, Dr. Olivier Klein

Visiting Scientists and Research Affiliates

Theodore M. Lyszczarz,[1] Paul M. Mankiewich,[2] David C. Shaver,[1] Shalom Wind[3]

Graduate Students

David Abusch-Magder, David J. Goldhaber-Gordon, Nicole Y. Morgan

2.1 Goals and Objectives

Sponsors

Joint Services Electronics Program
 Grant DAAH04-95-1-0038
National Science Foundation
 Grant ECS 92-03427
U.S. Army Research Office
 Grant DAAH04-94-G-0119

When electrons are confined to a small particle of metal or a small region of semiconductor, both the energy and charge of the system are quantized. In this way such nanometer-sized systems behave like artificial atoms.[4] The quantization of energy is familiar: The solutions of the Schrodinger equation in an isolated region have discrete energies. In some ways, however, the quantization of charge is more mysterious. We are quite comfortable with the idea that the charge of a collection of electrons is discrete. However, the charge in any small volume of a large sample of conductor is *not* discrete because the electronic wavefunctions are extended over the entire sample. Only when the states are localized is the charge quantized.

Artificial atoms have been constructed using metals and semiconductors, and they have been given a variety of names: single-electron-tunneling transistor, quantum dot, single-electron transistor, and zero-dimensional electron gas. The physics of all these devices is the same, although the limits in which they operate may be quite different. The goal of our research is to better understand the physics of these devices in order to optimize their performance so that circuit design may commence.

2.2 Summary of Recent Work

Our work this year has been successful in two arenas. First, we have followed up our studies, reported one year ago,[5] showing that electrons in a single-electron transistor in GaAs undergo phase transitions as a function of magnetic field. We have recently reported the observation of low energy excitations which correspond to the critical fluctuations of these transitions. Second, we have recently fabricated metal oxide silicon SETs (MOSSETs) which show single electron phenomena up to 20 K. We concentrate here on the latter research.

A single-electron transistor (SET) is an island of charge which is coupled to leads by tunnel barriers. There are two energies that are encountered in changing the electronic state of the SET: the energy required to add an electron to the island, U, and the energy required to excite the electrons already on the island, ΔE. Both these energies increase as the size of the island is diminished. Since the resolution of single electron phenomena is limited by the temperature of the electrons, we may increase the operating temperature by

---

1 MIT Lincoln Laboratory, Lexington, Massachusetts.

2 AT&T Bell Laboratories, Short Hills, New Jersey.

3 IBM Corporation, Thomas J. Watson Research Laboratories, Yorktown Heights, New York.

4 M.A. Kastner, "Artificial Atoms," *Phys. Today* 46(1): 24 (1993).

5 O. Klein, C. de C. Chamon, D. Tang, D.M. Abusch-Magder, S.-G. Wen, M.A. Kastner, and S.J. Wind, "Exchange Effects in an Artificial Atom at High Magnetic Fields," *Phys. Rev. Lett.* 74: 785 (1995).

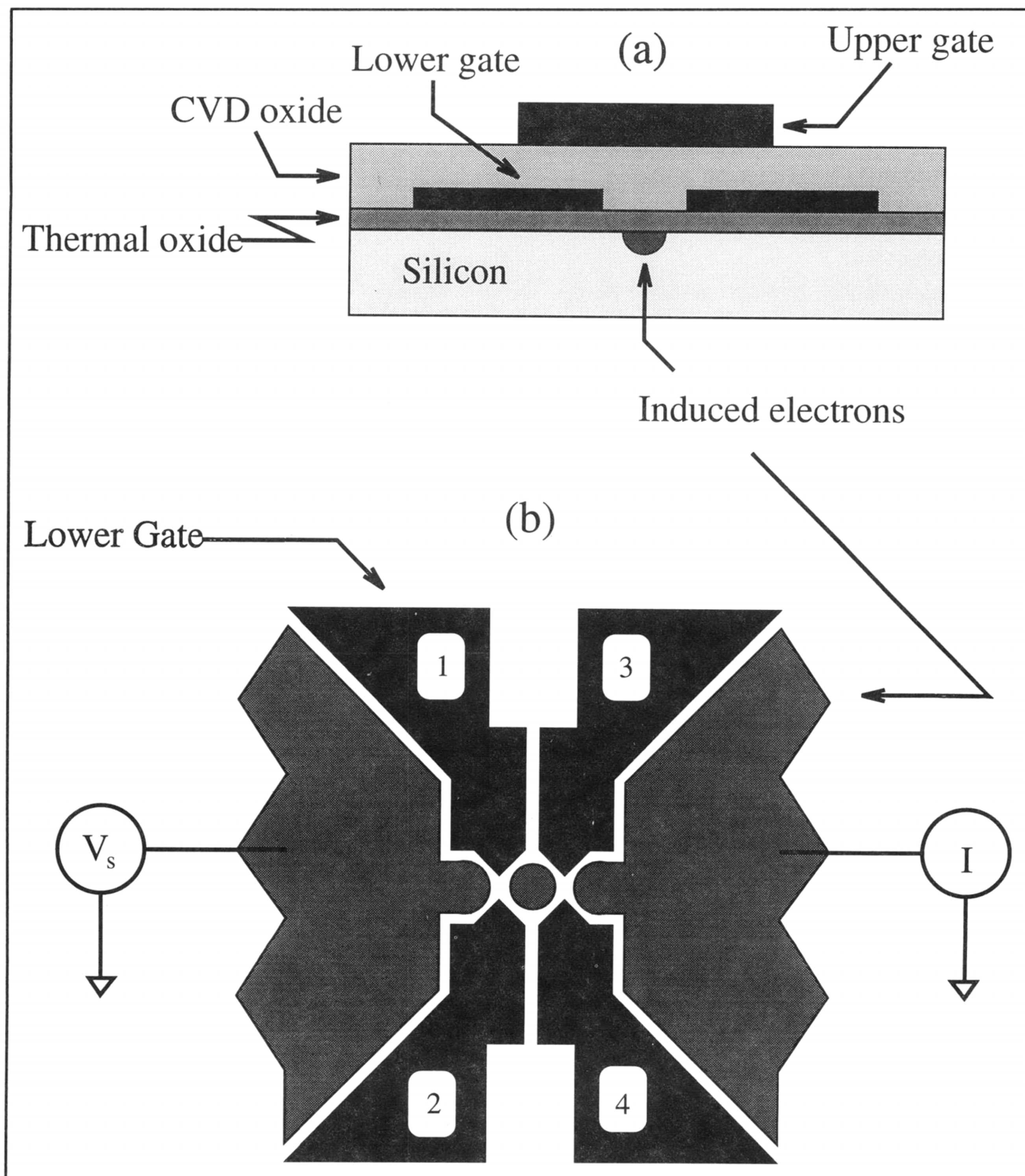

Figure 1. Schematic of the device: (a) The cross section shows the p-silicon substrate with 20 nm thermal SiO_2, lower metal gate patterned by electron beam lithography and liftoff, chemical vapor deposited SiO_2, and upper gate. In standard operation, the upper gate is held at a voltage above the inversion threshold while the voltages on the lower gates are kept below threshold. Electrons are then induced at the Si-SiO_2 interface where the lower gate does not screen the field of the upper gate. (b) Sketch of a top view of our device with an isolated island of electrons coupled to two leads by tunnel junctions. The lead on the left is the source and is biased at V_s; the lead on the right, called the drain, is connected through an ammeter to ground. Our measurements are made by biasing the source and measuring the current that flows to the drain.

reducing the size of the SET. The purpose of our work is to fabricate small SETs and, in addition to achieving higher operating temperatures, to exploit the improved relative resolution to explore coherent interaction between the electrons in the leads and the electrons on the island.

An island of charge can be created by electrostatic depletion of a two-dimensional electron gas (2DEG). By changing the voltages on metallic gates which lie a short distance above a 2DEG, the electrostatic fields can be adjusted; in this way, both the number of electrons on the island and the size of the tunnel barriers may be varied. The size of the island is limited by the depletion width, which decreases as the gates are brought closer to the 2DEG; a small depletion width allows the possibility of a small island. Thus, to make small SETs one needs a material system in which the gates can be brought close to the 2DEG. The Si-SiO_2 MOS system is ideal for this purpose because SiO_2 is a robust insulator; layers as thin as 10 nm have low leakages, high breakdown voltages, and are easily fabricated. We have therefore chosen to fabricate SETs in the silicon MOS system, rather than in the more extensively studied GaAs-AlGaAs system. Previously observed coulomb blockade (CB) effects in electrostatically patterned MOS structures have resulted from impurities. More recent work[6] has achieved CB in a Si-SiO_2 system using pattern-dependent oxidation. However, our studies are the first showing well-defined CB phenomena in lithographically defined MOSSETs where the tunnel barriers are created by gate electrodes.

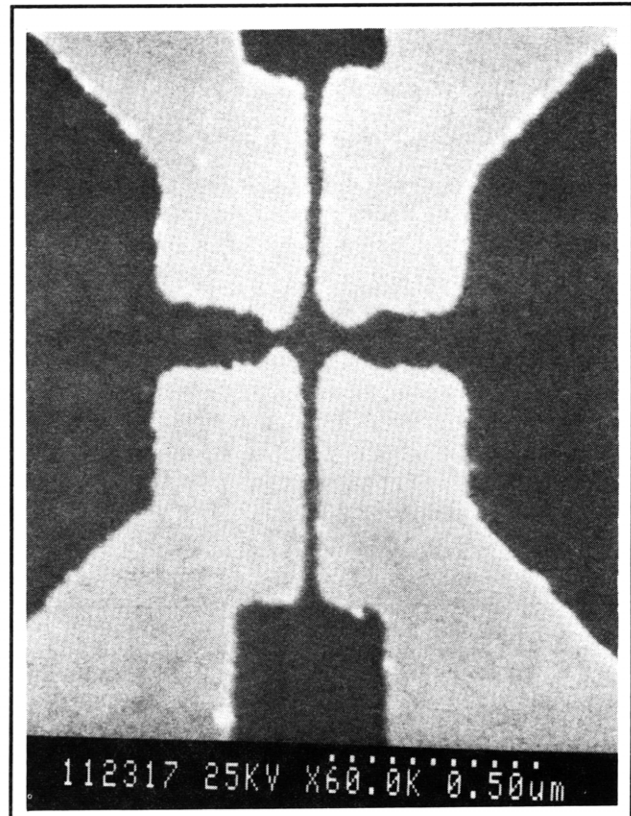

Figure 2. A scanning electron micrograph is shown of one of our SETs. Note that the gap between gates 1 and 3 is 25 nm. The full diameter of the gap between the lower gates is 120 nm. The measurements discussed in this paper were made on a larger SET whose diameter is about twice as large.

2.3 Fabrication

Standard silicon fabrication techniques have been used in combination with electron beam lithography to fabricate MOSSETs, thus taking advantage of existing technology. Figure 1a shows the basic layer structure of our devices. We start with a lightly doped p-silicon substrate (25-45 Ω cm) and grow a 20 nm thick dry thermal oxide on its surface. Using electron beam lithography, we pattern a 50 nm layer of PMMA, which then serves as a lift-off mask for our lower metal gate, a 20 nm layer of chromium. A scanning electron micrograph of a typical lower metal gate pattern is shown in figure 2. After chemical vapor deposition of 85 nm of SiO_2 on top of the gate structure, we anneal our sample at 900 degrees C for 30 seconds in dry nitrogen. The upper metal gate and interconnects are then deposited by sputtering aluminum and are patterned photolithographically. Ohmic contact to the inversion layer is made by degenerately doped n^+ implants.

In standard operation, the upper metal gate is held at a voltage above the inversion threshold while the voltages on the lower metal gates are kept below threshold. Electrons collect at the Si-SiO_2 interface in regions where the upper gate potential is not screened by the lower metal gates (see figure 1b); in this way, it is possible to pattern the 2DEG into an isolated island of electrons coupled to leads by tunnel junctions. Because this device uses SiO_2, which is a robust insulator, we can apply large voltages to the gates: > 20 V can be applied to the lower gates, while 50 V can be applied between the upper and lower gates. The relative transmission of the tunnel barriers can be tuned by applying a

[6] Y. Takahashi, M. Nagase, H. Namatsu, K. Kurihara, K. Iwadate, Y. Nakajima, S. Horiguchi, K. Murase, and M. Tabe, "Fabrication Technique for Si Single-Electron Transistor Operating at Room Temperature," *Electron. Lett.* 31: 136 (1995).

voltage difference of up to 2 V between left and right lower gates.

2.4 Results

We have observed periodic conductance oscillations resulting from CB in a MOSSET, with an addition energy U = 15 meV, which corresponds to temperature $T = U/k_B$ = 175 K. Figure 3 shows the conductance as a function of upper gate voltage for several temperatures in a MOSSET whose lithographic diameter is approximately 250 nm. We see the periodic peaks in conductance typical of CB with a spacing of 200 mV. One of the most striking features of our data is that the conductance peaks persist to high temperatures: the traces in figure 3 are taken at 0.315 K, 6 K, and 20 K with an offset added for clarity. The peaks are still well resolved at 6 K, and there is a clear periodic modulation of the conductance which persists up to 20 K, consistent with a CB charging energy of 175 K.

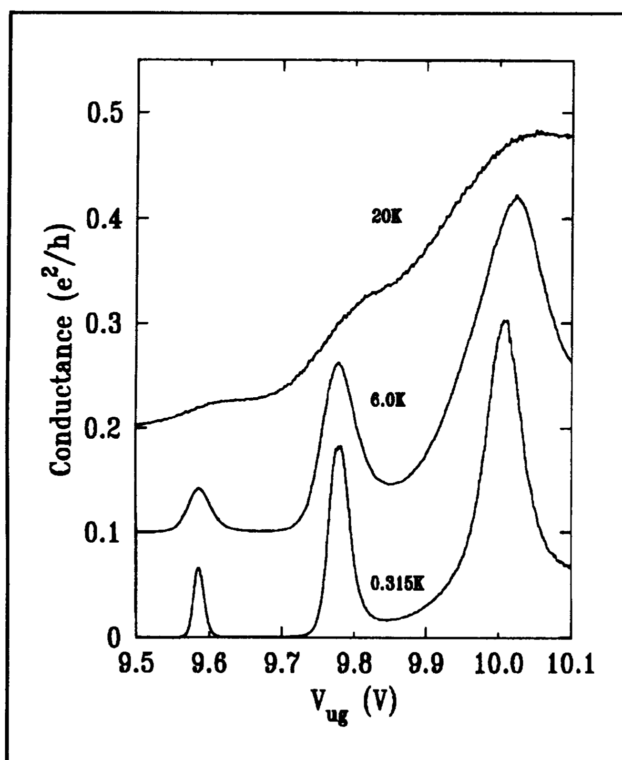

Figure 3. The conductance as a function of upper gate voltage is shown here for three different temperatures. Note that the conductance peaks are still sharp at 6 K, while a periodic modulation of the conductance is still present even at 20 K. This is consistent with a charging energy corresponding to 175 K. The measurement was made using standard lock-in techniques at 8.7 Hz with an excitation voltage of 65 μV for the traces at 6 K and 20 K and an excitation voltage of 20 μV for the trace at 0.315 K. The excitation voltage in all our measurements was chosen to be less than k_BT/e so that we measure the linear response of the system. The curves at 6 K and 20 K are offset by $0.1e^2/h$ and $0.2e^2/h$ for clarity; the curve at 6 K is shifted by 0.06 V to the left.

There are four important energy scales that determine the transport in CB: ΔE is the typical excitation energy of the island with a fixed number of electrons; Γ is the lifetime broadened natural line width resulting from tunneling between the island and the leads; U is the charging energy of the island; and k_BT is the temperature of the SET. To observe well-separated CB peaks, $k_BT < U/5$. Past studies of SETs have been restricted to two different regimes, both of which have $k_BT > \Gamma$. For metal SETs, where $k_BT > \Delta E$, theory predicts that a conductance peak has full width at half maximum FWHM = 4.2 k_BT/α, where $\alpha = C_g/C_\Sigma$, the ratio of the gate capacitance to the total capacitance. The amplitude is predicted to be independent of temperature. In the other previously studied regime, $k_BT < \Delta E$, and the transport is dominated by tunneling though a single quantum state. Again the FWHM is linear in temperature, but is now given by 3.5 k_BT/α, while the peak amplitude varies as $1/T$. Thus, by examining both the amplitude and width of the peaks as a function of temperature we may determine both the transport regime and the factor α.

In our data, we find that the width of the peak at 9.8 V is linear in temperature (figure 4a). However, in contrast to the prediction of the simplest model, the width extrapolates to a finite value at T=0. This result suggests that our MOSSET is operating in the regime where $\Gamma > k_BT$. In this regime, we expect the line shape to be a convolution of the natural line shape of the zero-temperature conductance resonance with the derivative of the Fermi-Dirac distribution function. If the line shape is Lorentzian with FWHM = Γ, the width is predicted to be linear in temperature, with a finite intercept: FWHM = $(3.5k_BT + \Gamma)\alpha$, which agrees well with the behavior seen in figure 4a. As discussed below, we find that Γ = 1.3 meV, corresponding to a temperature of 15 K, for the peak at 9.8 V. Furthermore, in this regime the amplitude is expected to have a $1/T$ dependence for $k_BT > \Gamma$, and below this temperature the amplitude is expected to saturate. Figure 4b shows such a crossover in the amplitude of the peak at 9.8 V, providing further evidence that the finite intercept in figure 4a is due to a large natural line width.

From the slope of the peak width versus temperature (figure 4a), we estimate α = 0.08. The physical meaning of α is simple: when the gate potential is changed by ΔV_g, the potential of the electron island is changed by $\alpha\Delta V_g$. We thus use α to convert the gate voltage periodicity of CB peaks to an energy scale: $U = e\alpha\Delta V_g$ = 15 meV, or U/k_B =

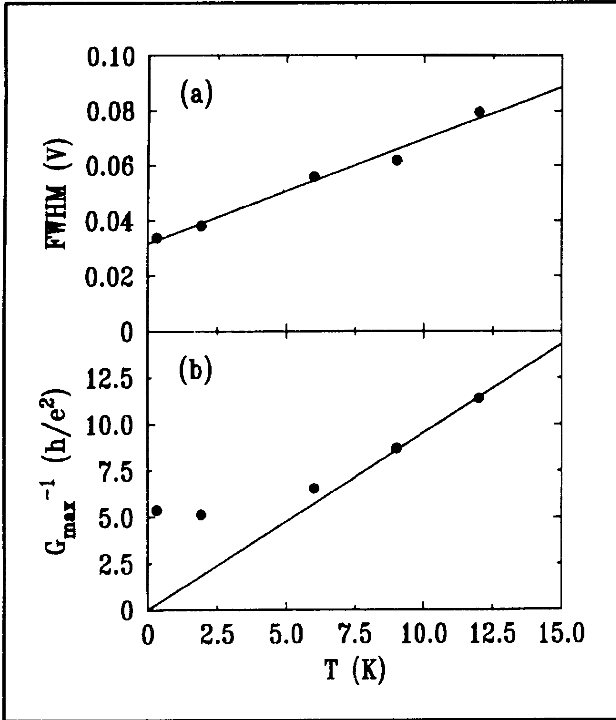

Figure 4. The full width at half maximum (a) and the inverse of the peak height (b) are shown as functions of temperature for the conductance peak at an upper gate voltage of 9.8 V (see figure 3). Notice that the width does not have a zero intercept, while the inverse of the maximum conductance saturates at low temperature. This behavior is results from the large natural line width G of the state. The line in (a) is a fit to all the points, while the line in (b) fits the high temperature points with a zero intercept.

175 K. Similarly, we use α to convert the peak widths and find Γs of 500 μeV, 1.3 meV, and 3.3 meV for the three peaks in figure 3, in order of ascending gate voltage.

We have also measured the differential conductance dI/dV_s as a function of V_s the source voltage, which we call the tunneling spectrum. This spectrum (shown in figure 5) is proportional to the density of single-particle states on the island which couple to the leads. The first feature to notice in figure 5 is the CB gap around zero bias. In addition, there are several features whose spacing is reproducible; these are marked with arrows. We associate these features in the density of states with excited states of the artificial atom (SET). The first peak in the spectrum on the right of the plot (arrow labeled gs N) is the current contribution from the ground state of the island with N electrons, while additional features (arrow labeled exc) are due to excited states of the N-electron island. Similarly, the peak on the left of the plot (arrow labeled gs N-1) is due to current through the ground state of the N-1-electron island.

The typical energy spacing of bound states in the SET is ~ 4 meV; we have converted the voltage axis in figure 5 into an energy scale by accounting for the capacitive coupling between the lead and the island. This large value reflects the very small spatial extent of the electron droplet. Furthermore, this direct measurement of ΔE confirms that $k_BT < \Delta E$, as we have seen in the temperature dependence data.

2.5 Publications

Kastner, M.A. "Mesoscopic Physics with Artificial Atoms." *Comments on Condensed Matter Physics.* Forthcoming.

Kastner, M.A., O. Klein, C. de C. Chamon, D. Tang, D.M. Abusch-Magder, U. Meirav, X.-G. Wen, and S.J. Wind. "Exchange Effects in Artificial Atoms." *Jpn. J. Appl. Phys.* 34: 16 (1995).

Klein, O., C. de C. Chamon, D. Tang, D.M. Abusch-Magder, S.-G. Wen, M.A. Kastner, and S.J. Wind. "Exchange Effects in an Artificial Atom at High Magnetic Fields." *Phys. Rev. Lett.* 74: 785 (1995).

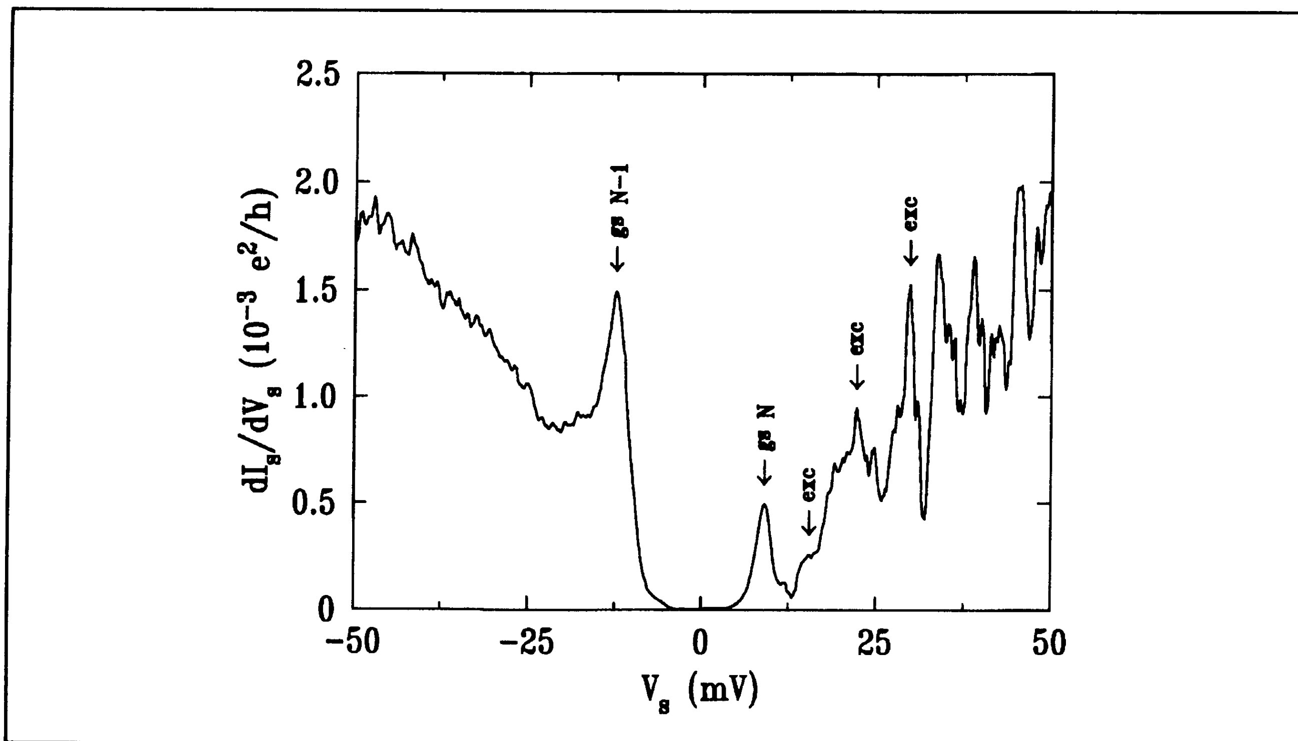

Figure 5. Tunneling spectrum of the SET at T = 0.315 K. The peaks correspond to variations in the density of states of the island. Peaks marked gs are due to tunneling through the ground state, while those marked exc are due to tunneling through excited states. The measurement was made using a lock-in amplifier at 8.7 Hz with an excitation voltage of 26 μV.